



Effect of cobalt metal loading on Fischer–Tropsch synthesis activities over Co/ γ -Al₂O₃ catalysts: CO conversion, C₅₊ productivity, and α value

Jung-Il Yang¹ · Chang Hyun Ko²

Received: 10 July 2018 / Accepted: 27 April 2019
© Springer Nature B.V. 2019

Abstract

This study investigates the effect of cobalt loading (5–20 wt% Co) on the physical properties of the alumina support and cobalt particle size of Co/ γ -Al₂O₃ catalysts for Fischer–Tropsch synthesis (FTS) reaction ($T=210$ °C (set), $P=20$ bar, $H_2/CO=2$). To characterize the catalysts and correlate these characteristics with their catalytic activities in FTS, N₂ adsorption, inductively coupled plasma, X-ray diffraction (XRD), transmission electron microscopy (TEM), and X-ray photoelectron spectroscopy (XPS) studies were conducted. N₂ adsorption and XRD analyses showed that as the cobalt loading was increased up to 15 wt%, the number of cobalt oxide particles increased by the direct interaction between cobalt oxide and the alumina support surface, but that when the cobalt loading was further increased to 20 wt%, the particle size of the cobalt oxide increased abruptly due to the additional cobalt loading on the previously loaded cobalt oxide. These physical properties of the supported cobalt catalysts were attributed to the pore structure of the alumina support. From the TEM micrographs, the size of cobalt particles was roughly estimated to increase from 20 to 50 nm at a cobalt loading up to 15 wt% Co/ γ -Al₂O₃ to 70–100 nm at 20 wt% cobalt loading. For the 5–15 wt% Co/ γ -Al₂O₃ catalysts, CO conversion and C₅₊ liquid oil productivity increased with increasing cobalt loading because they were strongly proportional to the number of cobalt particle active sites. However, the 20 wt% Co/ γ -Al₂O₃ catalyst showed the highest value of α because the larger cobalt particles increased the opportunity for chain growth. The XPS data also supported the greater reducibility of the cobalt species in 20 wt% Co/ γ -Al₂O₃ and hence its larger size compared to that at low cobalt loading.

Keywords Fischer–Tropsch synthesis · Co/ γ -Al₂O₃ · Cobalt loading · CO conversion and C₅₊ liquid oil productivity · α value

✉ Jung-Il Yang
yangji@kier.re.kr

✉ Chang Hyun Ko
chko@jnu.ac.kr

Extended author information available on the last page of the article

Introduction

Clean liquid fuels can be manufactured from synthesis gas, a mixture of H_2 and CO, which is produced from reforming, and/or shift reaction, or gasification of methane, coal, and biomass [1]. Potential world oil shortage is strongly pushing the development of alternative technologies for the manufacture of transportation fuels. Furthermore, as these fuels contain no aromatics, sulfur, or nitrogen-containing compounds, their high purity will easily satisfy the upcoming stricter environmental regulations in both Europe and the USA [2, 3].

Fischer–Tropsch synthesis (FTS) is used to convert synthesis gas into synthetic liquid fuels and is, therefore, a crucial technology for gas-to-liquid (GTL) process. Although many metals exhibit FTS activity, only cobalt (Co) and iron (Fe) catalysts are in industrial use [4, 5]. These two catalysts share the following similarities in FTS: they are very active, produce a wide range of long-chained hydrocarbons, and afford a product distribution that follows the Anderson–Shultz–Flory equation [5]. However, cobalt is active in its Co metal form and iron is active as Fe carbides [5, 6]. Cobalt catalysts, although much more expensive than iron, are used in smaller amounts and can be recycled for several years by regeneration (oxidation/reduction) [5, 7]. Cobalt catalysts have been used for FTS because of their high activity towards the production of long-chained hydrocarbons, wax, and long catalyst life about 10-fold longer than Fe [7–9]. Currently, cobalt catalysts are used in commercial GTL plants of Oryx GTL by Sasol/QP and Pearl GTL by Shell [10]. In the FTS reaction, Sasol has developed a Co-based slurry bubble column reactor (SBCR) with a capacity of 34,000 bpd and Shell has been developing a Co-based fixed-bed reactor (FBR) with a capacity of 140,000 bpd [10, 11]. Therefore, there are strong efforts for the optimization and tailoring of cobalt catalysts for specific applications [1].

Martinez et al. reported the influence of cobalt loading, cobalt precursor, and promoters on the physico-chemical and catalytic properties of Co/SBA-15 catalysts for the FTS reaction [12]. The Co/SBA-15 catalysts supported the preferred formation of C_{5+} hydrocarbon because of its high reducibility, while the less reducible, low-cobalt-loading sample exhibited a product distribution shifted toward the formation of lighter hydrocarbons (methane, C_2 – C_4). Storsøter et al. investigated the performance of unpromoted and Re-promoted cobalt catalysts supported on γ - Al_2O_3 , SiO_2 , and TiO_2 in terms of mass transfer limitations and the structural parameter, χ [13]. They reported that the χ values for these catalysts were all in the range 7 – $52 \times 10^{16} \text{ m}^{-1}$ and that the reaction rates and selectivities should not be limited by the diffusion of CO to the active sites. Furthermore, although the reactants were in the gas phase, the support pores were filled with liquid products, and diffusion in the liquid phase was several orders of magnitude slower than that in the gas phase. Barbier et al. observed the size sensitivity of cobalt particles in the FTS reaction, in which the intrinsic activity and the chain growth probability, α , firstly increased and then stabilized with increasing particle size [14]. They also reported the efficient control of cobalt reducibility as one of the key issues in the design of highly active cobalt alumina-supported

FTS catalysts. Blanchard et al. reported the successful use of the cobalt catalyst for the production of alcohols so long as both metallic cobalt and cobalt oxide were in a close association within the cobalt catalyst [15]. Furthermore, considering CO diffusional restrictions within the catalyst, an eggshell cobalt catalyst was developed for increasing FTS rates and C_{5+} selectivity [16]. Further research has examined the dependency of the FTS activity on the reducibility of cobalt catalysts. Jacobs et al. investigated the support, loading, and promoter effects on the reducibility of the catalysts and found that alumina support, increased cobalt loading, and addition of Ru, Pt, and Re were favorable for improving the reducibility of the catalysts [17]. The promoting effect of MnO was attributed to the lower degree of cobalt reduction because the manganese retards cobalt reduction [18]. The chain growth probability increased, and the product distribution shifted toward olefinic products at increased MnO loadings. Furthermore, the catalyst life and contaminants tolerance of the cobalt catalysts used in FTS are important due to their relatively high cost. Although the oxidation of nano-sized metallic cobalt to cobalt oxide during FTS has been considered a major deactivation mechanism [19–21], van de Loosdrecht reported that oxidation can be ruled out as a major deactivation mechanism [22]. Oxidation has also been eliminated as a potential deactivation mechanism of cobalt crystallites ≥ 6 nm supported on alumina. In their recent research on the poisoning of cobalt catalyst used for FTS, Sparks et al. reported that a H_2S level of about 500 ppb was the threshold for a detectable decrease in activity [23]. Recently, Farzanfar et al. reported inorganic complex precursor route for preparation of high-temperature Fischer–Tropsch synthesis Ni–Co nanocatalysts and they showed that the novel procedure was more advantageous than impregnation and co-precipitation methods for the preparation of effective and durable cobalt catalysts for Fischer–Tropsch synthesis [24]. Also, Hajjar et al. investigated the effect of applying nanoporous graphene to Fischer–Tropsch synthesis catalysts [25]. The novel catalysts, Co/graphene oxide and Co/nanoporous graphene, yielded heavier hydrocarbons compared with the Co/ Al_2O_3 catalyst, possibly due to the high surface area and intrinsic properties of the carbon nanostructures as effective hydrogen carriers.

This work investigates the catalytic activities of Co/ γ - Al_2O_3 catalysts in FTS according to the cobalt loading. In particular, N_2 adsorption, inductively coupled plasma (ICP), X-ray diffraction (XRD), transmission electron microscopy (TEM), and X-ray photoelectron spectroscopy (XPS) studies are conducted to characterize the cobalt catalysts according to the cobalt loading and to correlate these catalyst characteristics with their catalytic activities in FTS. Especially, the influence of cobalt loading (5–20 wt%) on the distribution of liquid oil products is discussed in terms of the chain growth probability, α . Finally, we investigate the effects of the number and size of cobalt active sites in the cobalt catalysts on the FTS activities in terms of CO conversion, C_{5+} productivity, and α value.

Experimental

Preparation of catalysts

Metallic cobalt supported on γ -Al₂O₃ (Co/ γ -Al₂O₃) supports were prepared as catalysts at four cobalt concentrations (5, 10, 15, and 20 wt%) by the wet impregnation of cobalt nitrate (Co(NO₃)₂, Aldrich) on γ -Al₂O₃. After impregnation, these samples were calcined at 400 °C for 8 h to obtain cobalt oxide supported on γ -Al₂O₃ (Co₃O₄/ γ -Al₂O₃). Prior to reaction, these samples were pre-reduced in situ with a hydrogen flow of 300 ml/min for 16 h at 350 °C to obtain Co/ γ -Al₂O₃.

Characterization of catalysts

XRD patterns for Co/ γ -Al₂O₃ and Co₃O₄/ γ -Al₂O₃ catalysts were obtained in the 2 θ range from 20° to 80° at intervals of 0.02° using a Rigaku Diffractometer (D/MAX Ultima III) with Cu K α radiation at 40 kV and 40 mA. TEM images of the Co/ γ -Al₂O₃ catalysts were obtained by Technai F30S-Twin (FEI) microscopy with an operating voltage of 300 kV. The surface areas of catalysts were measured by N₂ adsorption at 77 K using ASAP2010 (micrometrics). The cobalt composition in the catalyst was measured by ICP-atomic emission spectroscopy (ICP-AES) using Optima 4300™ DV ICP-OES (PerkinElmer). The oxidation states of the cobalt in the catalyst were investigated by XPS (MultiLab2000 by VG) using AlK α radiation (1486.6 eV).

Catalytic experiments

The FTS reaction was carried out in a conventional, tubular FBR with a diameter of 25.4 mm and a length of 300 mm. A schematic diagram of the experimental apparatus is shown in Fig. 1. Reaction heat was supplied by an electrical furnace with a PID controller (Hanyoung Science). The reaction temperature was monitored by a thermocouple (*K* type, nickel-chromium vs. nickel-aluminum, Omega Engineering, Inc.) installed at the lower end of the catalyst bed through the inlet of the reactor. Mass flow controllers (Brooks, 5850E) were used for precise flow control of the reactants (H₂/CO=2 molar ratio) under pressurized reaction conditions by a back pressure regulator (Tescom). The liquid products were completely recovered by a cold trap working with a cold ethylene glycol (0 °C) circulating system, which was finally collected from the product reservoir. The total flow of gas products and unreacted reactants was measured by using a dry gas meter (Shinogawa, 1 L/rev) and the products gas was sampled to analyze the gas composition by using an on-line sampler located after the dry gas meter.

Reactant and product analysis

The product distribution in the liquid products was analyzed by a simulated distillation (SIMDIS) technique using the ASTM D2887 method. A gas chromatograph

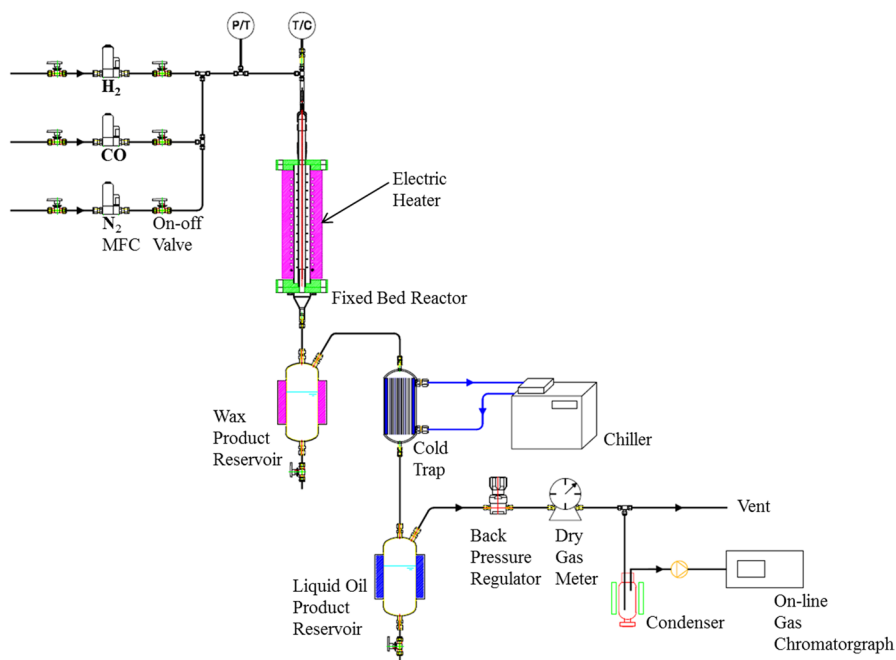


Fig. 1 Schematic diagram of the experimental apparatus for Fischer–Tropsch synthesis (FTS) reaction

(Agilent 6890 series) equipped with a SIMDIS 2884 column (Analytical Controls) and an auto injector system was used for analysis. The compositions of both gas products and reactants were analyzed by using a gas chromatograph (HP5890 GC) equipped with a Carboseive II column. Furthermore, the details of reactant and product analysis have been comprehensively explained in our previous study [26].

Results and discussion

Effect of cobalt loading on the physical properties of the supported catalysts

Table 1 lists the chemical composition and textural properties (BET surface area, total pore volume, and average pore diameter), as obtained by N_2 adsorption, of pure γ -alumina and the four supported cobalt catalysts according to the cobalt loading. The cobalt loading influenced the surface area and pore volume of the catalysts. The surface area and pore volume of the catalyst linearly decreased as the cobalt loading was increased from 5 to 15 wt%, which Martinez et al. attributed to a partial blockage of the support pores by cobalt oxides cluster and/or partial collapse of the porous structure with the increase of cobalt loading. Therefore, the increased cobalt loading may be related with the interaction between cobalt oxide and the alumina support surface [12]. On the other hand, as the cobalt loading was increased from the 15–20 wt%, the surface area, pore volume, and average pore diameter remained

Table 1 Chemical composition and textural properties obtained by N₂ adsorption of pure γ -alumina and supported cobalt catalyst

Catalyst	Co (wt%)	S_{BET} (m ² /g)	Total pore volume (cm ³ /g)	Average pore diameter (nm)
γ -Al ₂ O ₃	–	144	0.22	60
5 wt% Co/ γ -Al ₂ O ₃	5.0	122	0.20	65
10 wt% Co/ γ -Al ₂ O ₃	9.4	119	0.18	61
15 wt% Co/ γ -Al ₂ O ₃	12.5	100	0.16	64
20 wt% Co/ γ -Al ₂ O ₃	16.6	100	0.16	64

unchanged, which indicated that the 15 wt% cobalt loading was sufficient for the complete coverage of alumina surface with cobalt oxide and the complete filling of pores in alumina support. Increasing the cobalt loading to 20 wt%, did not further affect the interaction between the cobalt oxide and the surface of the alumina support, but it did increase the size of the previously loaded cobalt oxide particles in the alumina support.

Effect of cobalt loading on cobalt particle size

As metallic cobalt is the active site for FTS reaction, the particle size of metallic cobalt is an important factor for catalytic activity [27]. However, measuring the particle size of metallic cobalt in a catalyst is relatively difficult because cobalt is immediately oxidized to cobalt oxide upon air exposure, even in ambient condition. Thus, the cobalt particle size was estimated indirectly by measuring the size of the cobalt oxide particles after the calcination step in the preparation of Co/ γ -Al₂O₃. As shown in Fig. 2, Co₃O₄ was the only phase detected in the XRD patterns for the cobalt species after this calcination step, and the other peaks were assigned to γ -Al₂O₃. The full width at half maximum (FWHM) peak for cobalt oxide reflects the particle size of the corresponding cobalt oxide. Storsøter et al. used the most intense Co₃O₄ peak, $2\theta = 36.9^\circ$, to calculate the Co₃O₄ particle size [13]. Especially, the XRD pattern of 5 wt% Co/ γ -Al₂O₃ presented only small broad cobalt oxide peaks in a pattern that was very similar to that of the pure γ -Al₂O₃ support. As the cobalt loading was increased to 15 wt%, the Co₃O₄ peak of $2\theta = 36.9^\circ$ clearly appeared and its size gradually increased, which was mainly attributed to the increased number of cobalt oxide particles as the cobalt loading was increased to 15 wt% in the alumina pores because of the interaction between cobalt oxide and the alumina support surface.

However, when the cobalt loading was further increased to 20 wt%, the peak of cobalt oxide at $2\theta = 36.9^\circ$ sharply increased, as shown in Fig. 2e. Therefore, it can be deduced that the particle size of cobalt oxide increased abruptly at this 20 wt% cobalt loading due to the effect of this additional cobalt loading on the previously loaded cobalt oxide.

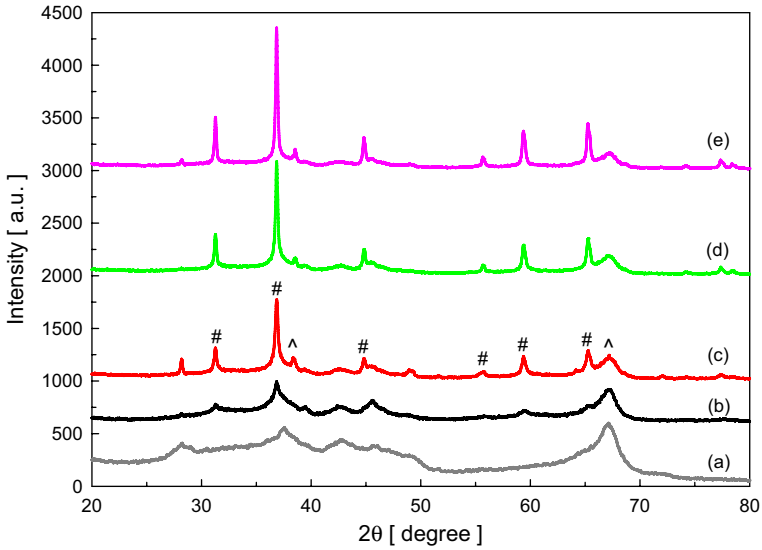


Fig. 2 X-ray diffraction (XRD) patterns for **a** γ -alumina, **b** 5 wt% Co/ γ -Al₂O₃, **c** 10 wt% Co/ γ -Al₂O₃, **d** 15 wt% Co/ γ -Al₂O₃, and **e** 20 wt% Co/ γ -Al₂O₃ after calcination at 400 °C for 8 h. Phases denoted are (#) cobalt oxide (Co₃O₄), and (^) γ -alumina

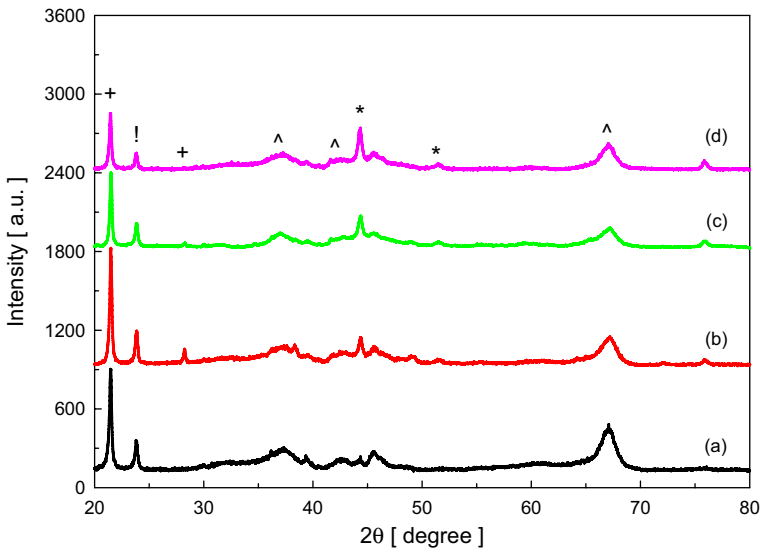


Fig. 3 X-ray diffraction (XRD) patterns for **a** 5 wt% Co/ γ -Al₂O₃, **b** 10 wt% Co/ γ -Al₂O₃, **c** 15 wt% Co/ γ -Al₂O₃, and **d** 20 wt% Co/ γ -Al₂O₃ after FTS reaction. Phases denoted are (*) metallic cobalt, (+) cobalt carbide (CoC₈), (!) aluminum cobalt carbide (AlCo₃C), and (^) γ -alumina

After the FTS reaction, the $\text{Co}/\gamma\text{-Al}_2\text{O}_3$ catalysts were retained for further XRD measurement. Figure 3 displays the XRD patterns of the four $\text{Co}/\gamma\text{-Al}_2\text{O}_3$ catalysts after FTS reaction. Small and broad peaks corresponding to metallic cobalt appeared. The peaks' intensity and broadness (FWHM) suggested that 20 wt% $\text{Co}/\gamma\text{-Al}_2\text{O}_3$ had the largest metallic cobalt particles.

These results obtained from the XRD patterns agreed well with the previous BET results. The BET analysis suggested that the cobalt particle size should be sharply increased at 20 wt% cobalt loading due to the saturation of the alumina pore structure at the 15 wt% cobalt loading, i.e., the optimum cobalt loading was 15 wt% for particle size control. Finally, the trend in the cobalt particle size was more clearly explained by using the XRD analysis.

TEM images of the $\text{Co}/\gamma\text{-Al}_2\text{O}_3$ catalysts after FTS reaction confirmed the Co particle size, which was deduced from the XRD results. As shown in Fig. 4, the cobalt particle size, actually the metallic cobalt particles covered by cobalt

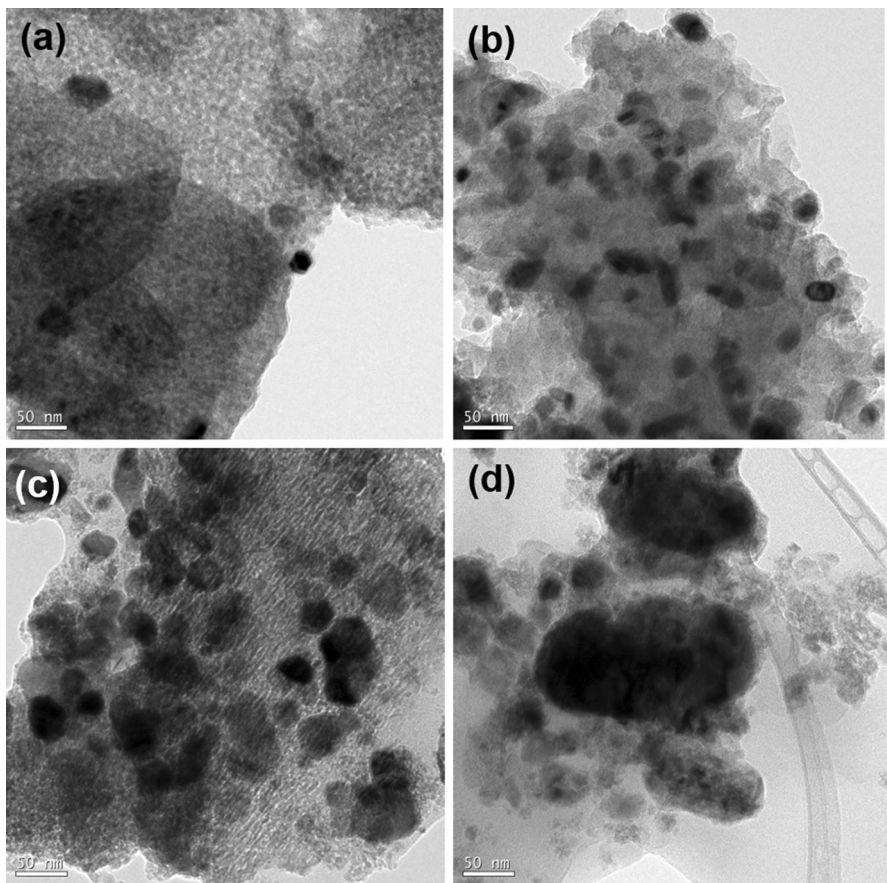


Fig. 4 Transmission electron microscopic (TEM) images of supported cobalt catalysts: **a** 5 wt% $\text{Co}/\gamma\text{-Al}_2\text{O}_3$, **b** 10 wt% $\text{Co}/\gamma\text{-Al}_2\text{O}_3$, **c** 15 wt% $\text{Co}/\gamma\text{-Al}_2\text{O}_3$, and **d** 20 wt% $\text{Co}/\gamma\text{-Al}_2\text{O}_3$ after FTS reaction

carbide, increased with increasing cobalt loading. The cobalt particles were roughly estimated to be sized 20–50 nm. Especially, the cobalt particle size increased drastically to 70–100 nm at 20 wt% cobalt loading. The cobalt particles began to agglomerate during the catalyst preparation due to the high cobalt precursor concentration.

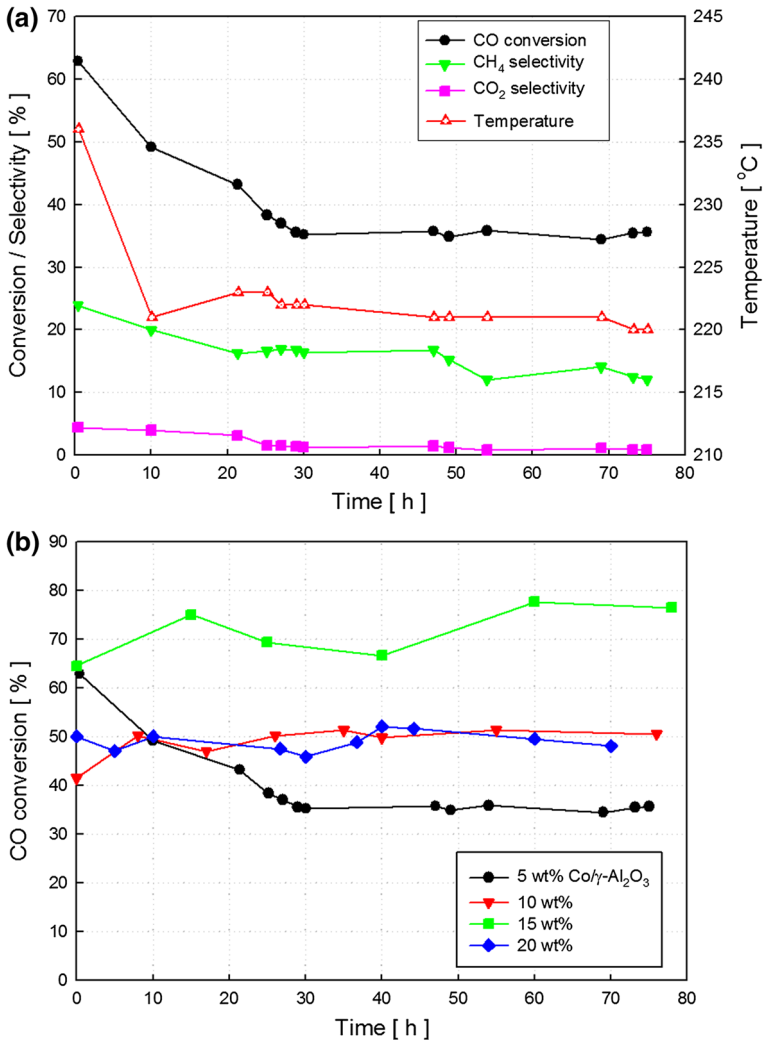


Fig. 5 Catalytic activities of 5 wt% Co/γ-Al₂O₃ (a) and CO conversion of 5 wt%, 10 wt%, 15 wt%, and 20 wt% Co/γ-Al₂O₃ catalysts (b) in a fixed bed reactor (FBR) for the FTS reaction (H₂/CO=2, F_{total}=100 ml/min, W_{cat}=4.5 g, P=2.0 MPa)

Performance of Co/ γ -Al₂O₃ catalysts

The catalytic activity of Co/ γ -Al₂O₃ at the four cobalt loadings, was investigated in an FBR under typical FTS conditions of 2.0 MPa, 210 °C (set), H₂/CO=2, and $W_{\text{cat}}/F=0.75 \text{ g}_{\text{cat}} \text{ h L}^{-1}$. Figure 5 shows the performance of the 5 wt% Co/ γ -Al₂O₃ catalyst during 80 h reaction. As shown in Fig. 5, the reaction temperature initially increased sharply to 236 °C due to the exothermic reaction heat generated in the FTS reaction, resulting in both high CO conversion and high CH₄ selectivity. After 30 h reaction, the following steady-state reaction activities were obtained: 36.4% CO conversion, 17.0% CH₄ selectivity, and 1.52% CO₂ selectivity at 217 °C. Furthermore, the C₅₊ selectivity was 36.5% and the C₅₊ liquid oil productivity reached 30.3 mL kg_{cat}⁻¹ h⁻¹. The chain growth probability, α , was calculated to be 0.839 based on the distribution of liquid oil products. The contact time (W_{cat}/F) of 0.75 g_{cat} h L⁻¹ for the 5 wt% Co/ γ -Al₂O₃ catalyst in the FTS reaction was confirmed as being acceptable for C₅₊ liquid oil production at 217 °C. It has previously been reported that the contact time is a critical point for controlling the internal mass transfer limitation induced by the produced hydrocarbons and that the liquid hydrocarbons produced during the short contact time block the pores of the catalyst, leading to catalyst deactivation [2, 28].

Table 2 summarizes the catalytic activities of Co/ γ -Al₂O₃ in the FTS reaction at the four cobalt loadings. CO conversion increased as the cobalt loading was increased up to 15 wt%, but then decreased at the higher cobalt loading of 20 wt%. This pattern of increasing and decreasing CO conversion was mainly ascribed to

Table 2 Effect of cobalt loading on the catalytic activities of Co/ γ -Al₂O₃ for FTS reaction in a fixed bed reactor (FBR)

Catalyst	5 wt% Co/ γ -Al ₂ O ₃	10 wt% Co/ γ -Al ₂ O ₃	15 wt% Co/ γ -Al ₂ O ₃	20 wt% Co/ γ -Al ₂ O ₃
Temp. (°C)	217	220	230	220
CO conv. (%)	36.4	50.1	74.2	48.6
Product sel. (%)				
CO ₂	1.52	11.0	9.80	9.92
CH ₄	17.0	32.3	29.3	28.3
C ₂ -C ₄	45.0	29.1	33.9	26.2
C ₅₊	36.5	27.6	26.9	35.6
Liquid oil productivity (ml kg _{cat} ⁻¹ h ⁻¹)				
Gasoline (C ₅ -C ₁₂)	15.4	26.1	49.0	24.8
Diesel (C ₁₃ -C ₁₈)	10.2	13.9	16.6	14.9
Wax (C ₁₉₊)	4.70	6.71	8.69	8.08
Total	30.3	46.7	74.3	47.8
Chain growth probabil- ity, α	0.839	0.834	0.831	0.855

the number of cobalt active sites provided by these catalysts. As described above in the catalysts characterization, the cobalt particle size in the Co/ γ -Al₂O₃ catalysts was unchanged at cobalt loading up to 15 wt%, as also supported by the XRD and TEM analyses (Figs. 2, 3, 4). Thus, the increase in the number of active sites in the catalysts may be directly related with the increase of cobalt loading. However, 20 wt% Co/ γ -Al₂O₃ actually offered fewer active sites than 15 wt% Co/ γ -Al₂O₃ because larger cobalt particles were formed in the preparation of 20 wt% Co/ γ -Al₂O₃.

The reaction temperature distribution was almost identical to the dependency of the CO conversion on the cobalt loading because FTS is a highly exothermic reaction and the generated reaction heat is proportional to the conversion.

Not only CO conversion, but also C₅₊ liquid oil productivity was proportional to the number of cobalt particles because those activities were closely related to the number of active sites. However, 20 wt% Co/ γ -Al₂O₃ showed the highest chain growth probability, α , as it was strongly related to the size of the cobalt active sites because larger cobalt particles afforded more chances for chain growth [14]. Furthermore, as the high reaction temperature was unfavorable for chain growth, the chain growth probability, α , and the C₅₊ liquid oil selectivity were inversely proportional to the reaction temperature for the similarly sized cobalt particles in the 5, 10, and 15 wt% Co/ γ -Al₂O₃ catalysts [14, 26].

The XPS data for the Co/ γ -Al₂O₃ catalysts after the FTS reaction are presented in Fig. 6. It was reported that the position of Co 2p_{3/2} peaks is related to the chemical status of the cobalt species [1]. Cobalt metallic species were identified using the Co 2p_{3/2} peak at 777.9 eV and the Co₃O₄ spinel phase was characterized by the Co 2p_{3/2} peak at 780.2 eV and a low intensity of the shake-up satellite peak at ca. 787 eV [1, 12,

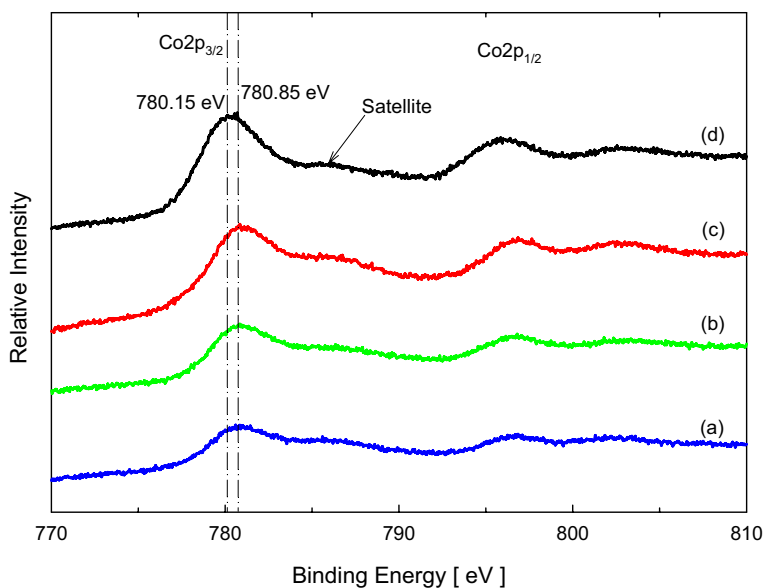


Fig. 6 Co 2p XPS spectra of the supported cobalt catalysts: **a** 5 wt% Co/ γ -Al₂O₃, **b** 10 wt% Co/ γ -Al₂O₃, **c** 15 wt% Co/ γ -Al₂O₃, and **d** 20 wt% Co/ γ -Al₂O₃ after FTS reaction

29]. For the 5, 10, and 15 wt% Co/ γ -Al₂O₃ catalysts, the binding energy of the Co 2p_{3/2} level was 780.85 eV, which decreased to 780.15 eV at the 20 wt% loading. This shift of the Co 2p_{3/2} peak toward a lower binding energy at the 20 wt% loading definitely implied that the cobalt species in 20 wt% Co/ γ -Al₂O₃ was more favorable for reducibility and larger than the others.

Conclusions

The following conclusions were derived from the results of the present work:

1. As the cobalt loading on the catalyst was increased from 5 to 15 wt%, the surface area and pore volume of the catalysts linearly decreased because of partial blockage of the alumina support pores by cobalt oxide cluster and/or partial collapse of the pore structure with increasing cobalt loading. However, at 20 wt% cobalt loading, the surface area, pore volume, and average pore diameter of the catalyst remained unchanged from the corresponding values of 15 wt% Co/ γ -Al₂O₃. Thus, the optimum cobalt loading was 15 wt% because the complete coverage of alumina surface with cobalt oxide and the complete filling pores in alumina was achieved at this loading.
2. XRD analysis revealed that the number of cobalt oxide particles increased as the cobalt loading was increased up to 15 wt% due to the interaction between cobalt oxide and the alumina support surface, whereas the particle size of the cobalt oxide increased as the cobalt loading was further increased to 20 wt% because of the additional cobalt loading on the previously loaded cobalt oxide. Furthermore, TEM analysis revealed cobalt oxide particle sizes of 20–50 nm and 70–100 nm at cobalt loadings of up to 15 wt% and 20 wt%, respectively.
3. As the cobalt loading in the Co/ γ -Al₂O₃ catalysts was increased from 5 to 15 wt%, both CO conversion and C₅₊ liquid oil productivity increased due to their high dependency on the number of cobalt particle active sites. However, the CO conversion and C₅₊ liquid oil productivity inversely dropped to 48.6% and 47.8 ml kg_{cat}⁻¹h⁻¹, respectively, at the high cobalt loading of 20 wt%, due to the increased cobalt particle size. Especially, the 20 wt% Co/ γ -Al₂O₃ catalyst showed the highest chain growth probability, α , because the larger cobalt active particles afforded more opportunities for chain growth. Furthermore, the XPS data also supported the more favorable reducibility of the cobalt species in 20 wt% Co/ γ -Al₂O₃, and hence its larger size compared to the other loadings.

Acknowledgements This work was supported by the Research and Development Program of the Korea Institute of Energy Research (KIER) (No. B9-2442-05).

References

1. W. Chu, P.A. Chernavskii, L. Gengembre, G.A. Pankina, P. Fongarland, A.Y. Khodakov, J. Catal. **252**, 215 (2007)
2. J.H. Yang, H.K. Kim, D.H. Chun, H.T. Lee, J.C. Hong, H. Jung, J.I. Yang, Fuel Process. Technol. **91**, 285 (2010)
3. M.H. Rafiq, H.A. Jakobsen, R. Schmid, J.E. Hustad, Fuel Process. Technol. **92**, 893 (2011)
4. M.E. Dry, Catal. Today **71**, 227 (2002)
5. I. Wender, Y. Zhang, L. Hou, J. Tierney, CFFS Annual Meeting, Roanoke, West Virginia, Aug. 1–4, 2004
6. H. Jung, J.I. Yang, J.H. Yang, H.T. Lee, D.H. Chun, H.J. Kim, Fuel Process. Technol. **91**, 1839 (2010)
7. C.G. Visconti, E. Tronconi, L. Lietti, P. Forzatti, S. Rossini, R. Zennaro, Topics Catal. **54**, 786 (2011)
8. R.L. Espinoza, Gas to Liquids (GTL). www.primethreelabs.com/assets/gtl.ppt
9. H. Schulz, Appl. Catal. A: Gen. **186**, 3 (1999)
10. A. Forbes, Gas to Liquids 2007, London, Oct. 30–31, 2007
11. R. Guettel, U. Kunz, T. Turek, Chem. Eng. Technol. **31**, 746 (2008)
12. A. Martinez, C. Lopez, F. Marquez, I. Diaz, J. Catal. **220**, 486 (2003)
13. S. Storsøeter, B. Totdal, J.C. Walmsley, B.S. Tanem, A. Holmen, J. Catal. **236**, 139 (2005)
14. A. Barbier, A. Tuel, I. Arcon, A. Kodre, G.A. Martin, J. Catal. **200**, 106 (2001)
15. M. Blanchard, H. Derule, P. Canesson, Catal. Lett. **2**, 319 (1989)
16. E. Iglesia, S.L. Soled, J.E. Baumgartner, S.C. Reyes, J. Catal. **153**, 108 (1995)
17. G. Jacobs, T.K. Das, Y. Zhang, J. Li, G. Racoillet, B.H. Davis, Appl. Catal. A: Gen. **233**, 263 (2002)
18. G.L. Bezemer, P.B. Radstake, U. Falke, H. Oosterbeek, H.P.C.E. Kuipers, A.J. van Dillen, K.P. de Jong, J. Catal. **237**, 152 (2006)
19. P.J. van Berge, J. van de Loosdrecht, S. barradas, A.M. van der Kraan, Catal. Today **58**, 321 (2000)
20. G. Jacobs, T.K. Das, P.M. Patterson, J. Li, L. Sanchez, B.H. Davis, Appl. Catal. A: Gen. **247**, 335 (2003)
21. G. Jacobs, P.M. Patterson, T.K. Das, M. Luo, B.H. Davis, Appl. Catal. A: Gen. **270**, 65 (2004)
22. J. van de Loosdrecht, B. Balzhinimaev, J.-A. Dalmon, J.W. Niemantsverdriet, S.V. Tsybulya, A.M. Saib, P.J. van Berge, J.L. Visagie, Catal. Today **123**, 293 (2007)
23. D.E. Sparks, G. Jacobs, M.K. Gnanamani, V.R.R. Pendyala, W. Ma, J. Kang, W.D. Shafer, R.A. Keogh, U.M. Graham, P. Gao, B.H. Davis, Catal. Today **215**, 67 (2013)
24. J. Farzanfar, A.R. Revani, Res. Chem. Intermed. **41**, 8975 (2015)
25. Z. Hajjar, M.D. Rad, S. Soltanli, Res. Chem. Intermed. **43**, 1341 (2017)
26. J.I. Yang, J.H. Yang, H.J. Kim, H. Jung, D.H. Chun, H.T. Lee, Fuel **89**, 237 (2010)
27. E. Iglesia, Appl. Catal. A: Gen. **161**, 59 (1997)
28. H.J. Kim, J.H. Ryu, H. Joo, J. Yoon, H. Jung, J.I. Yang, Res. Chem. Intermed. **34**, 811 (2008)
29. F. Morales, O.L.J. Gijzeman, F.M.F. de Groot, B.M. Weckhuysen, Stud. Surf. Sci. Catal. **147**, 271 (2004)

Publisher's Note Springer Nature remains neutral with regard to jurisdictional claims in published maps and institutional affiliations.

Affiliations

Jung-Il Yang¹ · Chang Hyun Ko²

¹ Clean Fuel Laboratory, Korea Institute of Energy Research, 152 Gajeong-ro, Yuseong-gu, Daejeon 305-343, Korea

² School of Applied Chemical Engineering, Chonnam National University, 77 Yongbong-ro, Buk-gu, Gwangju 500-757, Korea